Modeling and Control of Moisture Content in a Batch Fluidized Bed Dryer Using Tomographic Sensor

J.A Villegas, M. Li, S.R. Duncan, H.G. Wang and W.Q. Yang

Abstract— In this paper, the modeling and control of the moisture content of the particles in a batch fluidized bed dryer are studied. First, a lumped mechanistic model is developed to describe the heat and mass transfer between solid, gas and bubble phases and experimental validation shows that the model can be used to predict the particle moisture content and temperature profiles during the drying process in the bed dryer. By validating the model both with and without an insulator on the wall of the dryer, it is shown that the wall temperature has a major effect on the process. Feedback control of material moisture content in a bed dryer is studied with tomographic sensors included in the control loop. A controller is designed to achieve a desired drying rate for wet materials. Simulations show that it is possible to control the drying rate.

I. INTRODUCTION

Fluidized beds have been used for many years in the food, pharmaceutical and chemical industries for carrying out a wide range of chemical reactions and unit operations. One of the primary advantages of fluidized bed systems arises from the fact that the high turbulence created in the bed provides high heat and mass transfer, as well as complete mixing of the solids and gases within the bed.

Much work has been done to model and analyze both continuous and batch fluidized bed dryers [1], [2], [3], [4], [5], [6] and several studies have attempted to control the moisture content in a continuous fluidized bed dryer [7], [8]. However, it seems that little work has been done to control batch fluidized bed dryers. In fact, in many situations manual control procedures are used and it is also known that the majority of industrial dryers operate at low efficiency levels [9]. It is clear that the use of control tools allow to improve quality product and to decrease energy consumption.

This paper presents a mathematical model to describe the heat and mass transfer between solids, gas and bubble phases, which has been developed by Palancz [1] and Li and Duncan [3]. This model can be used to improve the operating conditions in both open and closed loop control. A simple control scheme has been designed to control the material moisture content in the bed dryer. Because of the difficulty in online measurement of moisture content, compared with temperature measurement, it is usually necessary to estimate the moisture from other measurements (e.g. temperature) by means of an observer. To overcome this problem, it

has been proposed to measure the moisture content online by electric capacitance tomography (ECT), which has been proved to give accurate moisture measurements [5]. This simplifies the control design process and as will be shown here, a simple (PI) control law can be designed which gives good performance under feedback control. One of the main advantages of ECT, apart of being fast, robust and non-invasive, is that it also contains information about other physical and chemical parameters making it ideal for use in distributed parameter control.

This paper is organized as follows. In Section II, the mathematical model describing the bed dryer is presented, followed by the model validation in Section III. A brief example of how to find optimal operating conditions is presented in Section IV. Section V describes a closed-loop approach. Finally, some conclusions and future work are discussed in Section VI.

II. MODEL DESCRIPTION

In this section we briefly present the mathematical model used to describe the mass and heat transfer between solid, gas and bubble phases in a batch fluidized bed dryer. This is based on a simple two-phase model [10] that includes a bubble phase and an emulsion phase consisting of an interstitial gas phase and a solid phase. The following are assumptions used to obtain the model:

1. In the bubble phase, gas moves upward as a plug flow.
2. In the bubble-gas phase, both the gas and the bubbles move upwards.
3. In the emulsion phase or dense phase, solids move downward.
4. All particles in the bed are uniform in size, shape and physical properties and have the same moisture content and temperature at any instant during the drying process.
5. The interstitial gas is perfectly mixed with the solid particles. There is heat and mass transfer between the interstitial gas and the other two phases: bubble and solid phases.
6. The bubble phase contains no particles and the clouds surrounding the rising bubbles are sufficiently thin that the bubble phase exchanges heat and mass only with the interstitial gas phase. The bubble size is assumed to be uniform and does not depend on the location within the bed. The gas in each bubble is perfectly mixed so that the moisture content and temperature are the same in the bubble. The moisture content and temperature in a bubble depends only on its position in the dryer.

J.A Villegas and S.R. Duncan are with the Department of Engineering Science, University of Oxford, Parks Road, Oxford OX1 3PJ, UK

M. Li is with the School of Pharmacy, De Montfort University, Leicester LE1 9BH, UK

H.G. Wang and W.Q. Yang are with the School of Electrical and Electronic Engineering, University of Manchester, PO Box 88, Manchester M60 1QD, UK

A. Mass and Energy Balance for Bubble Phase

It is assumed that as a bubble rises through the bed, its size and velocity remain constant with the bed height, while its moisture content and temperature change due to the exchange of mass and heat with the interstitial gas. This has been verified for the case $U_0 \geq 2U_{\mathrm{mf}}$ ([11]).

According to the simple two-phase model, the rising velocity of a single bubble relative to the emulsion phase and the absolute velocity of the bubble phase in the bed are given by

$$U_{br} = 0.711(gd_b)^{1/2} \quad \text{and} \quad U_b = U_0 - U_{mf} + U_{br}, \quad (1)$$

where the minimum fluidization velocity can be found from ([10])

$$\frac{1.75}{\varepsilon_{mf}^3}\left(\frac{d_p\mu_{mf}\rho_g}{\mu_g}\right)^2 + \frac{150(1-\varepsilon_{mf})}{\varepsilon_{mf}^3\xi^2}\left(\frac{d_p\mu_{mf}\rho_g}{\mu_g}\right)$$
$$= \frac{d_p^3\rho_g(\rho_w s - \rho_g)g}{\mu_g^2}. \quad (2)$$

The fraction of the bubble volume in the bed δ_b is given by

$$\delta_b = \frac{U_0 - U_{mf}}{U_b} \quad (3)$$

and the value of voidage of emulsion phase at the minimum fluidisation condition $\varepsilon_{\mathrm{mf}}$ can be calculated as

$$\varepsilon_{mf} = 0.586\xi^{-0.72}\left(\frac{\mu_g^2}{\rho_g(\rho_{ws}-\rho_g)gd_p^3}\right)^{0.029}\left(\frac{\rho_g}{\rho_{ws}}\right)^{0.021}. \quad (4)$$

1) Mass Balance:
The mass balance for the bubble phase in the control volume can be written as

$$U_b\frac{dx_b}{dz}(z) = K_{be}(x_e - x_b) \quad \text{with } x_b = x_0 \text{ at } z = 0. \quad (5)$$

The equation above can be integrated to find the analytical solution of the bubble moisture content ([3]), from which the average moisture content of bubbles along the vertical position of the fluidized bed dryer can be found as

$$\tilde{x}_b = x_e + (x_e - x_0)\frac{U_b}{K_{be}H_f}\left(\exp\left(-\frac{K_{be}}{U_b}H_f\right) - 1\right). \quad (6)$$

2) Energy Balance:
The steady state energy balance in the control volume leads to

$$\frac{dT_b}{dz}(z) = \left(\frac{H_{be}}{\rho_gU_b(c_g + c_{\mathrm{wv}}x_b)}\right)(T_e - T_b) \quad (7)$$

with $T_b = T_0$ at $z = 0$. The interchange coefficient of mass transfer between the bubble and interstitial gas phases K_{be} and the interchange coefficient of heat transfer between the bubble and interstitial gas phases H_{be} are given in [10] and [3].

B. Mass and Energy Balance for the Interstitial Gas Phase

The interstitial gas exchanges mass with both the bubble phase and solid particles. It also exchanges heat with the dryer wall.

1) Mass Balance:
The mass balance can be simplified as ([1], [3])

$$\rho_g\frac{U_{mf}}{H_f\delta_b}(x_e - x_0) = \rho_gK_{be}(\tilde{x}_b - x_e)$$
$$+ \frac{6(1-\varepsilon_{mf})(1-\delta_b)}{d_p\delta_b}\sigma(x_p^* - x_e) \quad (8)$$

2) Energy Balance:
The energy balance can be simplified as ([1], [3])

$$\frac{\rho_gU_{mf}}{H_f}(c_g + c_{\mathrm{wv}}x_0)(T_e - T_0) = \delta_bH_{be}(\tilde{T}_b - T_e)$$
$$+ \alpha_wh_w(T_w - T_e)$$
$$+ \frac{6\sigma}{d_p}(1-\varepsilon_{mf})(1-\delta_b)(T_p - T_e)\big(c_{\mathrm{wv}}\sigma(x_p^* - x_e) + h_p\big) \quad (9)$$

where the specific wall-surface for heat transfer is $\alpha_{ex} = S_w/V_{tot}$ and the space-average bubble-phase temperature is obtained from (7) as

$$\tilde{T}_b = T_e + (T_e - T_0)\frac{\rho_g(c_g + x_bc_{\mathrm{wv}})U_b}{H_{be}H_f}.$$
$$\left(\exp\left(-\frac{H_{be}}{\rho_g(c_g + x_bc_{\mathrm{wv}})U_b}H_f\right) - 1\right) \quad (10)$$

The coefficient of convective heat transfer between solids and gas is calculated by ([10])

$$\mathrm{Nu}_p = \frac{h_pd_p}{k_g} = 2 + 1.8\,\mathrm{Re}_p^{1/2}P_r^{1/3} \quad (11)$$

with

$$\mathrm{Re}_p = \frac{d_pU_0\rho_g}{\mu_g} \quad \text{and} \quad P_r = \frac{c_p\mu_g}{k_g}. \quad (12)$$

The evaporation coefficient is given by $\sigma = (h_p\rho_gD_g)/k_g$. Several methods are available to predict the heat-transfer coefficient between the interstitial gas and the dryer wall. Li and Finlayson ([12]) found that the best correlation for spherical packing is

$$h_w = 0.17\,\mathrm{Re}_p^{0.79}\frac{k_g}{d_p}. \quad (13)$$

C. Mass and Energy Balance for Solid Phase

1) Mass Balance:
Under normal drying conditions the moisture content of a solid particle decreases by evaporation of its moisture into the interstitial gas. The rate at which the moisture content decreases is given by

$$-\frac{\rho_s}{1 + \frac{\rho_s}{\rho_w}x_{pc}}\frac{d\tilde{x}_p}{dt} = \frac{6}{d_p}\sigma(x_p^* - x_e) \text{ with } \tilde{x}_p = x_{p0} \text{ at } t = 0. \quad (14)$$

2) Energy Balance: The energy balance for a particle can be simplified as ([1], [3])

$$\rho_s(c_p + \tilde{x}_p c_w)\frac{dT_p}{dt} = \left(1 + \frac{\rho_s}{\rho_w}x_{pc}\right)\frac{6}{d_p}\Big(h_p(T_e - T_p)$$
$$- \sigma(x_p^* - x_e)(c_{\text{wv}}T_e - c_w T_p + \gamma_0)\Big)$$
(15)

with the initial condition $T_p = T_{p0}$ at $t = 0$. In the equation above, γ_0 is the heat of vaporisation of water at a reference temperature $T_{\text{ref}} = 0$. The value of the moisture content of the saturated drying medium at the surface of the solid particle depends on the temperature and the moisture content of the particle, i.e.,

$$x_p^* = \Psi_1(T_p)\,\Psi_2(\tilde{x}_p)$$
(16)

where $\Psi_1(T_p)$ can be obtained from Mollier charts, and $\Psi_2(\tilde{x}_p)$ is a correction function depending on the character of the solid-moisture system. $\Psi_1(T_p)$ can be approximated by ([1])

$$\Psi_1(T_p) = 0.622\,\frac{P_w}{760 - P_w}\ \text{with}\ P_w = 10^{0.622 + \frac{7.5\,T_p}{238 + T_p}},$$
(17)

when $0 < T_p < 100^o C$. A drying process consists of two phases: a constant rate drying and a falling rate drying. During the constant rate phase the correction function $\Psi_2(\tilde{x}_p)$ can be set as ([2])

$$\Psi_2(\tilde{x}_p) = \begin{cases} 1 & \text{for } x_p \geq x_{pc} \\[2mm] \dfrac{\tilde{x}_p^n(x_{pc}^n + K)}{x_{pc}^n(\tilde{x}_p^n + K)} & \text{for } x_p < x_{pc} \end{cases}.$$
(18)

III. MODEL VALIDATION

The process model has been validated using data obtained from a Sherwood M501 fluidized bed dryer, where the wet product used is rice granules. Different tests were carried out and in particular the effect of the wall temperature was investigated. The wall is made of glass and first it was left without any insulation.

Equations (6), (8), (9), (10), (14) and (15), with appropriate boundary conditions, constitute the governing equations of the dynamic model of a batch fluidized bed dryer. To determine the moisture content and temperature profiles of solid particles in the dryer during a drying process, the set of first-order differential equations (14) and (15) were solved using a 4th order Runge-Kutta algorithm. At each time step, the moisture content x_p^* of the drying gas on the surface of particles is firstly calculated according to the temperature and the averaged moisture content of the particle (see equations (16)-(18)). Then the algebraic equations (6) and (8) are solved to determine the moisture contents of bubble and interstitial gas phases $\tilde{x}_b$ and x_e. The interstitial gas and the bubble gas temperature, T_e and $\tilde{T}_b$, can be calculated using equations (9) and (10). Finally the moisture content and temperature of solid particles are updated based on the calculated results.

$g = 9.81$	$k_g = 2.93 \times 10^{-2}$	$D_g = 2.1 \times 10^{-5}$
$n = 1.1$	$c_w = 4.19 \times 10^3$	$H_f = 0.56$
$\rho_g = 1$	$\mu_g = 2.1 \times 10^{-5}$	$\rho_s = 760$
$D_c = 0.16$	$\gamma_0 = 2.5 \times 10^6$	$c_g = 1.06 \times 10^3$
$K = 0.45$	$c_{\text{wv}} = 1.93 \times 10^3$	$c_p = 1.6919 \times 10^3$
$\rho_w = 1000$	$d_p = 2 \times 10^{-4}$	$d_b = 0.06$
$\xi = 1$	$x_{pc} = 16.5\%$	

A. Bed Dryer Without Wall Insulation

In order to predict the moisture and temperature profiles of the wet product in the dryer, the physical properties of the product and the geometrical parameters of the dryer have to be determined for use in the model. As most of the parameters are difficult to measure accurately in practice, approximations are made. Also, to predict both temperature and moisture content profiles, a compromise has to be made by adjusting the model parameters, such as the critical moisture content, effective bubble diameter, and the constants n and K in equation (18). A constant wall temperature assumption is not valid in this case, because a significant temperature increase of the dryer wall was observed during the drying process. Therefore, the wall temperature was measured and included in the simulations. The parameter values are shown in Table I.

In the test, the inlet air velocity was kept constant at $2.63\,m\,s^{-1}$ during the first 6 minutes after which it is reduced to $2.39\,m\,s^{-1}$. The inlet air temperature was fixed at $65\,^oC$. The initial moisture content (x_{p0}) was 25.81%, the initial particle temperature (T_{p0}) was $28.5\,^oC$ and the initial moisture content of the inlet air (x_0) was set to 1.1%. Comparison of the predicted temperature with the measurement is shown in Fig. 1, where it can be seen that the particle temperature profile is predicted accurately. The predicted moisture content profile is shown in Fig. 2, where again the model predicts its value accurately. It is concluded that the model can predict well the temperature and moisture content profiles when the wall temperature is known.

B. Bed Dryer with Insulated Wall

For the second set of tests, the dryer wall is assumed to be insulated. In this case there is heat exchange between the interstitial gas and the wall, but there is no heat exchange between the wall and the ambient. As expected, the drying process is faster than the non-insulated wall, and the final temperature reached by the product is higher (see Fig. 3). Also, in the same figure the moisture profile of the particles can be seen. To avoid measuring the wall temperature, the temperature profile is approximated by a first-order differential equation, which is obtained from the heat equation. To do this, the transfer function (which is irrational) of the heat equation from the inner wall temperature to the particle temperature is found and approximated by a first order transfer function, which in the Laplace domain is given
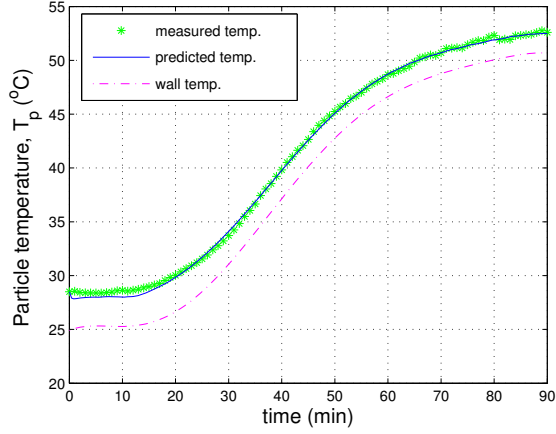
Fig. 1.   Particle and wall temperature.
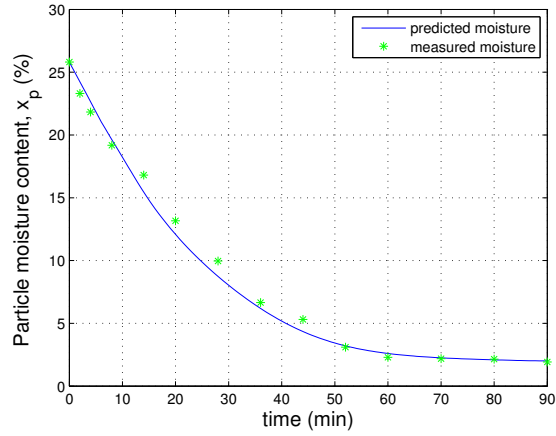
Fig. 2.   Moisture content in the particles.

by

$$T_w(s) = \frac{\alpha_w \mathrm{Bi}_w}{L_w s + \alpha_w \mathrm{Bi}_w} T_p(s) \qquad (19)$$

where $\alpha_w = 6 \times 10^{-7}\, m^2\, s^{-1}$ is the thermal diffusivity of the wall, $\mathrm{Bi}_w = 51.2$ is the Biot number of the wall, and $L_w = 4 \times 10^{-3}\, m$ is the width of the wall. In the simulation, the parameters given in Table I were used.

IV. OPTIMAL OPERATING CONDITIONS

One of the main advantages of having a mathematical model is that it allows to find optimal operating conditions. Typically the bed dryer is used as a "black-box" where the input variables (the inlet air velocity and temperature) are set to function in a pre-defined window of operation, which is usually not energy efficient. Based on the model presented in the previous section one could try to find optimal operating conditions. For instance, one could attempt to minimize the energy consumption in a batch drying. In a drying process, the energy input is mainly used to heat up the inlet air. Thus the energy consumption is proportional to the integral of the product of inlet air velocity and temperature and a
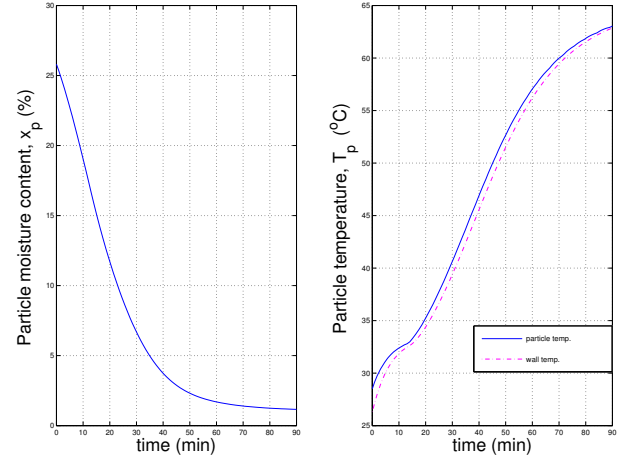
Fig. 3.   Moisture content and temperature in the particles with wall insulator.

performance index of a batch fluidized bed dryer can be defined as

$$J = \int_0^{t_f} c_g \rho_g A\, U_0(t) T_0(t)\, dt.$$

The optimal inlet air velocity and temperature can be determined by minimizing this performance index to achieve a specified final moisture content within a minimum drying time. The optimization is constrained by the allowable range of the manipulated variables (inlet air velocity and temperature), which can be cast as an optimization problem as follows

$$J_{\mathrm{opt}} = \min_{U_0, T_0, t_f} \int_0^{t_f} c_g \rho_g A\, U_0(t) T_0(t)\, dt$$

s.t.
$$(20)$$
$$\tilde{x}_p(t_f) \le \tilde{x}_{\mathrm{final}}$$
$$u_l \le U_0 \le u_u$$
$$T_l \le T_0 \le T_u$$

where the subscripts l and u denote the lower and upper bound, respectively, on the input variables. For the Sherwood M501 bed dryer the following bounds were set: $u_l = 0.3\, m\, s^{-1}$, $u_u = 3.5\, m\, s^{-1}$, $T_l = 50\, ^o\mathrm{C}$, $T_u = 85\, ^o\mathrm{C}$, and $\tilde{x}_{\mathrm{final}} = 2\%$. For this setting the optimal operating conditions were found. The Energy was reduced to $6.067 \times 10^7\, J$ (around 16% reduction), the final moisture content of 1.99% is reached after 50 min, and the optimal input values are shown in Fig. 4. This values can be preprogrammed in many bed dryers. In case smother input values are desired, the derivatives of these values can be included in the performance index, e.g.

$$J = \int_0^{t_f} c_g \rho_g A\, U_0(t) T_0(t) + w_1 \dot{U}_0(t) + w_2 \dot{T}_0(t)\, dt,$$

where w_1 and w_2 are weighting functions.
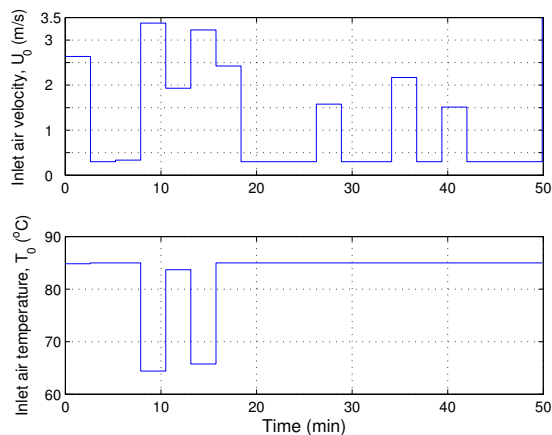
Fig. 4.   Optimal inlet air velocity and temperature.
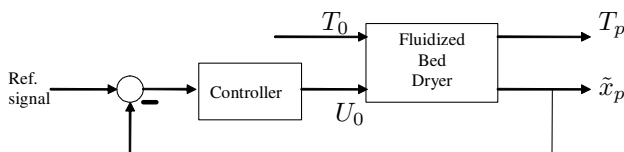
Fig. 5.   Control Loop.

V.   CONTROL OF FLUIDIZED BED DRYER

In most industrial processes, accurate moisture control of wet particles is required to improve the quality and consistency of the product. Because of the difficulty in measuring the moisture content directly, it is necessary to include the design of an observer in the control loop in order to estimate the moisture content from the measured temperature of the wet product. A better alternative is to measure the moisture content online by ECT, which has been proved to give accurate moisture measurements [5]. The frame of the ECT sensor is the wall of the fluidized bed and the ECT sensor is enclosed by an earthed shielding to eliminate external interference. There are 12 electrodes (4cm long and 2.5cm wide in average) around a cross section of the fluidized bed, see [5] for more details.

In the model parameter sensitivity analysis of batch fluidized bed dryers [3], it has been shown that the performance of a fluidized bed dryer is dominated by the inlet gas velocity rather than the inlet gas temperature (T_0). This suggests that the inlet gas velocity (U_0) can be chosen as the only manipulated variable for control, while the inlet gas temperature can be kept constant, see Fig. 5.

A PI (proportional plus integral) controller was designed to achieve a desired drying rate of wet materials. Simulation studies have been carried out to validate the proposed strategy. The batch fluidized bed dryer is simulated using the model described in Section II whose parameters are shown in Table I. The manipulated inlet gas velocity is constrained to lie in the range $0.3 \leq U_0 \leq 3.5$. Two different situations are considered in the simulations:
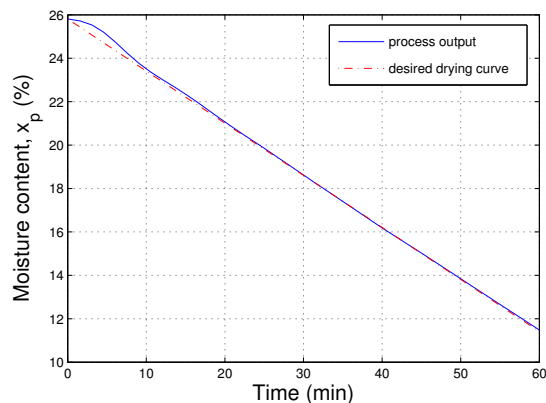
Fig. 6.   Moisture content using a PI controller.
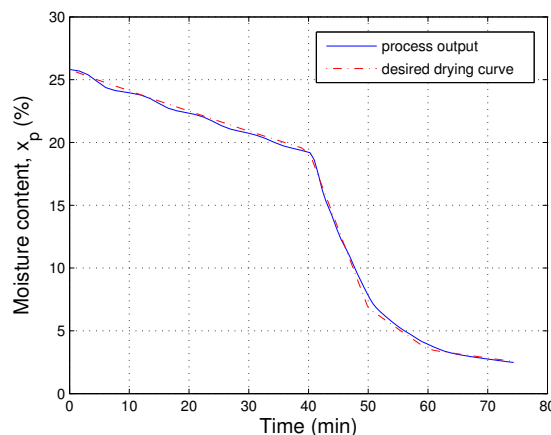
Fig. 7.   Moisture content using a PI controller and different drying rates.

1. First, the desired drying rate is set to a constant value of 4×10^{-5} per second. In this case, the proportional gain K_p is set to 100 and the integral gain K_I is set to $0.01\,s^{-1}$. Fig. 6 shows the output of the closed-loop system together with the desired drying curve. It can be seen that the particle moisture profile follows the desired drying curve with a drying rate of 4×10^{-5} per second.

2. In a second instance, the reference signal is set so that different desired drying rates are followed. In this case, the proportional gain K_p is set to 200 and the integral gain K_I is set to $0.05\,s^{-1}$. The output of the closed-loop system is shown in Fig. 7. Again, the output follows the desired drying curve with an average error less than 5%.

VI.   CONCLUSIONS AND FUTURE WORK

A dynamic model has been developed for a batch fluidized bed dryer. The experimental validation shows that the proposed lumped dynamic model can be used to predict the particle moisture content and the temperature profiles during the drying process. However, the simulations also show that the effect of the wall temperature has to be included in order

to obtain good predictions. It has also been shown that the use of this model allow to improve the efficiency of the bed dryer.

Feedback control of material moisture content in a bed dryer has also been studied and it is seen that including the measurement of the moisture content in the control loop simplifies the design process. A simple PI controller was designed and it is shown that it can be successfully used to control a batch fluidized bed dryer.

The model used in this paper is based on several assumptions which predict the dynamic behavior of the bulk moisture content in the bed dryer. However, in some applications it would be better to have a distributed parameter model and to apply feedback control to regulate spatial distribution of moisture content by manipulating the inlet air flow field. In this case, the tomographic sensors play a key role since they provide a reading of the moisture and solids distribution in the dryer. This approach is currently being studied.

NOMENCLATURE

A	Area of air distributor (m^2)
c_g	Heat of drying gas $(J\,kg^{-1}\,K)$
c_p	Heat of particles $(J\,kg^{-1}\,K)$
c_w	Heat of water $(J\,kg^{-1}\,K)$
c_{wv}	Heat of water vapor $(J\,kg^{-1}\,K)$
d_b	Effective bubble diameter (m)
d_p	Mean particle diameter (m)
D_c	Diameter of the bed column (m)
D_g	Diffusion coefficient of drying gas $(m^2\,s^{-1})$
g	Acceleration due to gravity $(m^2\,s^{-1})$
H_f	Height of bed (m)
h_p	Heat transfer coefficient between drying gas and solids $(J\,s^{-1}\,m^{-2}\,K^{-1})$
h_w	Heat transfer coefficient between drying gas and dryer wall $(J\,s^{-1}\,m^{-2}\,K^{-1})$
i_b	Enthalpy of gas bubbles $(J\,kg^{-1})$
i_{we}	Enthalpy of water vapor in emulsion gas $(J\,kg^{-1})$
Nu	Nusselt number
k_g	Thermal conductivity of drying gas $(J\,s^{-1}\,m^{-1}\,K^{-1})$
Pr	Prandtl number
Re	Reynolds number
T	Temperature
U_0	Inlet gas superficial velocity $(m\,s^{-1})$
U_b	Gas superficial velocity in bubble phase $(m\,s^{-1})$
U_{br}	Linear velocity of a bubble $(m\,s^{-1})$
U	Velocity $(m\,s^{-1})$
x	Moisture content (kg/kg)
$\tilde{x}$	Average moisture content (kg/kg)
x_p^*	Moisture content of drying gas on surface of a particle

Greek symbols

ε	Void fraction
γ_0	Heat of vaporization $(J\,kg^{-1})$
δ_b	Fraction of bubble
μ_g	Viscosity of gas $(kg\,m^{-1})$
ρ	Density $(kg\,m^{-3})$
σ	Evaporation coefficient $(kg\,m^{-2}\,s^{-1})$
ξ	Sphericity of particles

Subscripts

g	Gas phase
e	Emulsion phase
b	Bubble
p	Particle
s	Solids
mf	Minimum fluidization

REFERENCES

[1] B. Palancz, "A mathematical model for continuous fluidized bed drying," *Chem. Eng. Sci.*, vol. 38, pp. 1045–1059, 1983.

[2] F. Lai, Y. Chen, and L. Fan, "Modelling and simulation of a continuous fluidized-bed dryer," *Chem. Eng. Sci.*, vol. 41, pp. 2419–2430, 1986.

[3] M. Li and S. Duncan, "Dynamical model analysis of batch fluidized bed dryers," *Submitted to Chem. Eng. Sci*, 2006.

[4] S. Syahrul, I. Dincer, and F. Hamdullahpur, "Thermodynamic modelling of fluidized bed drying of moist particles," *International Journal of Thermal Sciences*, vol. 42, pp. 691–701, 2003.

[5] H. Wang, W. Yang, P. Senior, R. Raghavan, and S. Duncan, "Investigation of batch fluidised bed drying by mathematical modelling, CFD simulation and ECT measurement," *Submitted to AIChE J.*, 2007.

[6] H. Wang, T. Dyakowski, P. Senior, R. Raghavan, and W. Yang, "Modelling of batch fluidised bed drying of pharmaceutical granules," *Chem. Eng. Sci.*, vol. 62, pp. 1524–1535, 2007.

[7] N. Abdel-Jabbar, R. Jumah, and M. Al-Hai, "State estimation and state feedback control for continuous fluidized bed dryers," *Journal of Food Engineering*, vol. 70, pp. 197–203, 2005.

[8] S. Temple, S. Tambala, and A. van Boxtel, "Monitoring and control of fluid-bed drying of tea," *Control Engineering Practice*, vol. 8, pp. 165–173, 2000.

[9] P. Dufour, "Control engineering in drying technology: Review and trends," *Drying Technology*, vol. 24, pp. 889–904, 2006.

[10] D. Kunii and O. Levenspiel, *Fluidization Engineering*. Butterworth-Heinemann, 1991.

[11] D. Bukur, C. Wittman, and N. Amundson, "Analysis of a model for a nonisothermal continuous fluidized bed catalytic reactor," *Chem. Eng. Sci*, vol. 29, pp. 1173–1192, 1974.

[12] C. Li and B. Finlayson, "Heat transfer in packed beds - a revaluation," *Chem. Eng. Sci.*, vol. 32, pp. 1055–1066, 1977.